Steel and Composite Structures, *Vol. 20, No. 6 (2016) 1193-1203*
DOI: http://dx.doi.org/10.12989/scs.2016.20.6.1193

Analytical evaluation of a modular CFT bridge pier according to directivity

Dongwook Kim *, Chiho Jeon [a] and Changsu Shim [b]

Department of Civil Engineering, Chung Ang University, Seoul, Republic of Korea

(*Received September 16, 2015, Revised December 03, 2015, Accepted February 11, 2016*)

Abstract. This paper focuses on the analytical behavior of modular circular concrete-filled tubular (CFT) column with enhanced bracing details. To design a full-scale bridge pier of multiple circular concrete-filled tubes, numerical analysis was used to evaluate structural performance according to load directivity. In previous research (Ma *et al*. 2012, Shim *et al*. 2014), low cycle fatigue failure at bracing joints was observed, so enhanced bracing details to prevent premature failure are proposed in this analysis. The main purpose of this research is to investigate seismic performance for the diagonal direction load without premature failure at the joints when the structure reaches the ultimate load. The ABAQUS finite-element software is used to evaluate experimental performance. A quasi-static loading condition on a modular bridge pier is introduced to investigate structural performance. The results obtained from the analysis are evaluated by comparing with load–displacement responses from experiments. The concrete-filled tubes with enhanced bracing details showed higher energy dissipation capacity and proper performance without connection failure for a diagonal load.

Keywords: modular bridge pier; CFT; non-linear analysis; quasi static; bracing

1. Introduction

Concrete-filled steel tubes (CFT) provide many structural merits in terms of their strength-to-weight ratio, high compressive and tensile strength, high ductility, and high resistance. Recently, CFT columns have been used widely in the main structural members of structures owing to their numerous merits. Despite these advantages, they may remain unexploited owing to the lack of guidelines on multiple columns for bridge piers. The application of multiple CFT modular piers is limited in terms of many variables that need to be resolved including strength, stiffness, connection details, and seismic design.

In previous research on modular bridge piers, a small-scale bridge pier with a diameter of 165.2 mm and a thickness of 6.0 mm was fabricated and tested to investigate behavior (Shim *et al*. 2014, Ma *et al*. 2012). The height of the pier was 3.0 m. The strong and weak axes for column spacing were 1.0 m and 0.8 m, respectively. From the test results, premature failure at the welding joints of the upper bracings was observed before the CFT columns reached yielding. To improve the

*Corresponding author, Ph.D. Candidate, E-mail: clearup7@cau.ac.kr
[a] Master Student, E-mail: chihobeer@cau.ac.kr
[b] Professor, E-mail: csshim@cau.ac.kr

 ISSN: 1229-9367 (Print), 1598-6233 (Online)

seismic performance of bridge piers, premature failure at joint connections must be prevented. To enhance seismic performance without premature failure, a full-scale test specimen having a height of 7.95 m with enhanced bracing details (BRB) is fabricated and tested. From the test results under the quasi-static loading condition, premature failure at the joints is not observed for the loading of the strong axis. Buckling-restrained bracings are used widely in seismic areas for both architectural engineering and rehabilitation of structures. BRBs and CFT columns have high and stable energy dissipation capacities, as shown in many experimental and analytical studies using moment frame system (Gu *et al*. 2014, Stefan 2012, MagarPatil *et al*. 2015, Hu *et al*. 2010, ElAawady *et al*. 2012).

In this paper, a new modular bridge column system with enhanced bracing details is evaluated through an analytical approach and experiments conducted on a full-scale test specimen to prevent connection failures. The main objectives are (1) verification of the structural performance of modular bridge pier with enhanced bracing details through FEM analysis; (2) evaluation of seismic performance in the diagonal direction.

2. Analysis model properties

The analysis is conducted using a model composed of five independent but interrelated components. Circular CFT columns had a 508 mm outer diameter with a 12 mm thickness. Bracing hollow steel tubes had 138 mm outer diameters with 12 mm thickness.

In this model, brace spacing between columns on the strong axis is 2.5 m. Fig. 1 shows the 7,950 mm height (including the footing and pier cap) modular CFT column analysis specimen having a 508.2 mm column diameter. Measuring the length of the column from the top of the foundation (5,800 mm) to the level of lateral loading, the aspect ratio of a single CFT column is 11. The column specimen consists of three layers of six braces and a pier cap module. The column module is 5,830 mm tall, including the part of the column embedded into the footing. The pier cap is rectangular and its dimensions are 5,500 mm × 3,000 mm. Its height is 1,900 mm.

Total height of the pier modular system is 5.2 m to the top of the footing. Multiple CFT columns were embedded into the footing with 1.5 times (770 mm) depth of the CFT diameter with studs anchored by welding. Longitudinal and transverse spacing of the columns are 2.5 m and 2.0 m, respectively. Three layers of six braces are designed to connect the column.

Concrete with a design cylinder compressive strength of 40 MPa is used. Structural steel tubes for circular CFT columns and braces have a yield strength and tensile strength of 315 MPa and 490 MPa, respectively. The analysis model consists of a CFT column module, a pier cap module, and footing module.

In general, CFT material provides many merits compared with other kinds of materials such as ordinary steel or reinforced concrete. It provides good interaction between the steel tube and the concrete, construction efficiency, fire resistance, and the highest confinement effect on the concrete core. Confining concrete provides not only increased confinement stress but much greater ultimate strain compared to the unconfined. As a result, the confining effect provides higher stiffness with ductile deformation.

In this research, C3D8R elements for the concrete core and the steel tube are used as they are the most suitable, and are applied to all materials. In terms of the steel part of the CFT, an elastic-perfectly-plastic model is applied, allowing for isotropic yield. If the stresses are below the yield surface, the behavior of the steel tube is linearly elastic: if the stress points reach the yield surface,

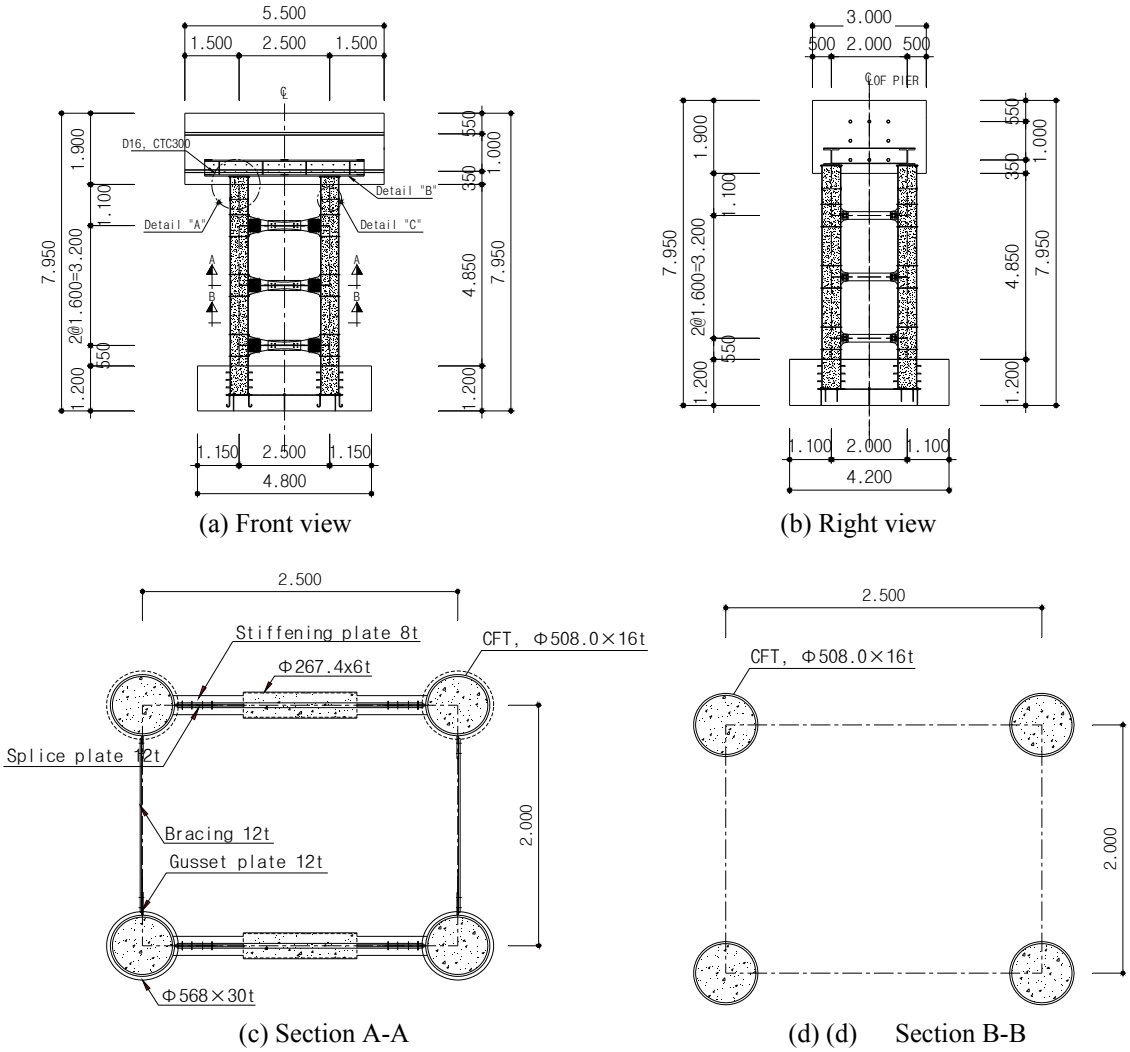

(a) Front view (b) Right view

(c) Section A-A (d) (d) Section B-B

Fig. 1 Analysis specimen

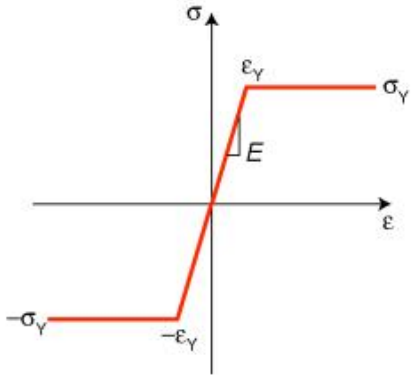

Fig. 2 Elastic-perfectly plastic stress-strain curve for steel (Ellobody *et al*. 2006)

Table 1 Stress-strain value for perfectly plastic and hardening plastic

Perfectly-Plastic		Hardening-Plastic	
Stress (MPa)	Strain	Stress (MPa)	Strain
315	0	315	0
315	0.03	315	0.014175
		490	0.098425

the behavior of the steel tube turns to perfectly-plastic. If loading is continued, the steel tube will eventually fail and will not be able to resist any further loading (Ellobody *et al*. 2006).

Poisson's ratio is chosen as 0.3 and the elastic modulus is equal to 210 GPa. Analysis is conducted for all the elements with a steel yield point at 315 MPa. Perfectly plastic material with no hardening is defined as shown in Fig. 2. Table 1 summarizes the perfectly plastic and hardening plastic strain, respectively.

In analysis, the concrete damaged plasticity model (CDPM) was chosen. This model features plasticity based on a continuum damage model. The CDPM is designed for applications in which concrete is subjected to monotonic, cyclic, and/or dynamic loading under low confining pressures. The CDPM consists of a combination of non-associated multi-hardening plasticity and scalar (isotropic) damaged elasticity to describe the irreversible damage that occurs during the fracturing process. The CDPM allows users to control stiffness recovery effects during cyclic load reversals. For these reasons the CDPM model was chosen for this analysis.

Using the sharing node method, surfaces of elements contact each other. Between two elements at the contact surface, nodes are set as sharing nodes automatically. This option allows each contact element to move when the structure deforms but does not allow penetration into each other.

Bridge piers are normally designed to support approximately 10% of their compressive strength. However, with the limits of the setup system, 1.8% of compressive axial force is applied by dead weight of the pier cap. In the analysis, axial load is not applied to the upper part of the complete structure to verify the effectiveness of the analysis model in the same conditions as in the

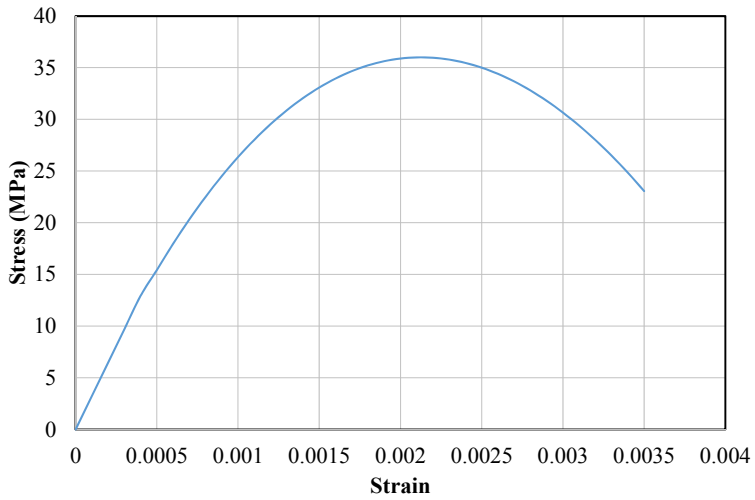

Fig. 3 Stress-strain curve for the concrete compression model

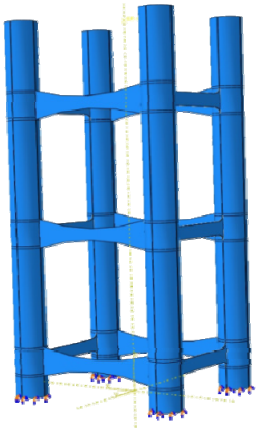

(a) Bottom constraint of the modular pier

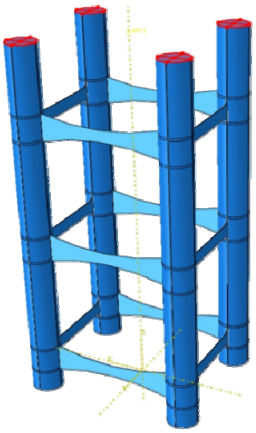

(b) Top constraint of the modular pier

Fig. 4 Boundary condition of modular pier

Table 2 Analysis model

Analysis model	Strong axis displacement (mm)	Weak axis displacement (mm)
S150W000	150	0
S150W045	150	45
S045W150	45	150
S000W150	0	150

Note: *S* = Strong axis; *W* = Weak axis

experiment. Two aspects of boundary conditions in the analysis model are taken into account. All degrees of freedom at the bottom surface of the CFT columns are disallowed. In addition, nodes at the top surfaces of the CFT columns are constrained as rigid bodies.

To verify the validity of the analysis model, load displacement curves and yield strain at the bottom part of the CFT columns are compared with those of the test results. Test results showed that 2,587 kN of maximum load corresponds to 134.04 mm of deformation. In the analysis, 134.04 mm of displacement is applied to the analysis model. The maximum load is 2,446 kN (134.04 mm), which shows a 5.45% difference in maximum load. Table 2 summarizes the analysis model according to the analysis parameters. The specimen labelled as S150W000 is subject to displacement control analysis; 150 mm displacement for the strong axis and 0 mm displacement for the weak axis. For the design of bridge piers under seismic action, Korean design codes specify the directivity of the loading condition. The loading parameters are considered as those of the Korean design specification.

3. Analysis results and discussion

3.1 Analysis for directivity

The ultimate load and ultimate displacement of the test results were 2,587 kN and 134.04 mm,

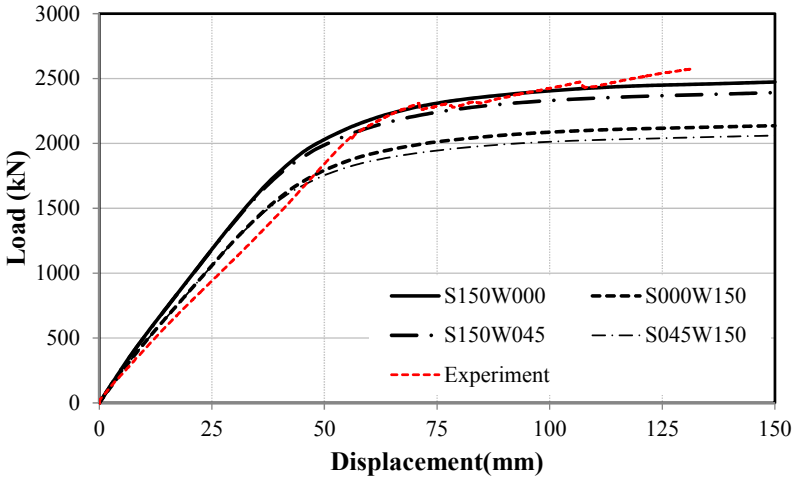

Fig. 5 Comparison of analysis results

respectively. In the analysis, 150 mm of displacement was introduced for the strong axis. The analysis specimen was modelled without pier cap segments. Therefore, it showed a 5.45% difference in initial stiffness because of differences in pure column lengths from their footings to their loading points. However, the global behavior showed reasonably good correlation as seen in Fig. 5.

A deformed shape and von Mises stress contour for the S150W045 and S000W150 specimens are shown in Fig. 6. Stress concentration was observed at the end of the CFT columns, and the bracing was still within the elastic range. As shown in Table 3, maximum load of the reference specimen (S150W000) was 2,470 kN while for the S000W150 specimen the value was 2,060 kN. The force introduced from the CFT column is transferred firstly to the bracing member. Then the force is transferred to the opposite side of the CFT column. This demonstrates that the change in the force transfer mechanism is being affected by the stiffness of bracing.

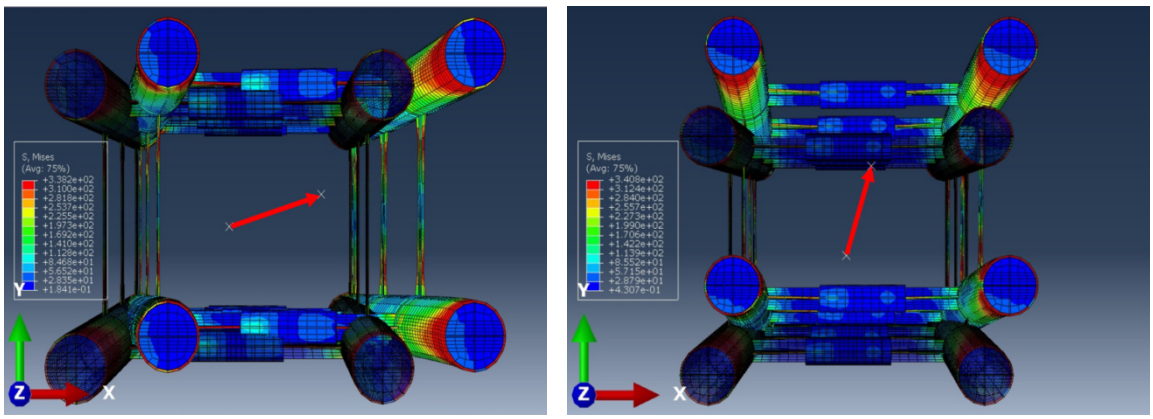

(a) von Mises stress of S150W045 (b) von Mises stress of S000W150

Fig. 6 Stress contour of analysis specimen

Table 3 Analysis results

Specimen	Maximum load (kN)	Comparison with reference specimen (%)
S150W000 (Reference specimen)	2,470 (Strong axis)	0
S150W045	2,390 (Strong axis)	-3
S045W150	2,140 (Weak axis)	-13
S000W150	2,060 (Weak axis)	-17

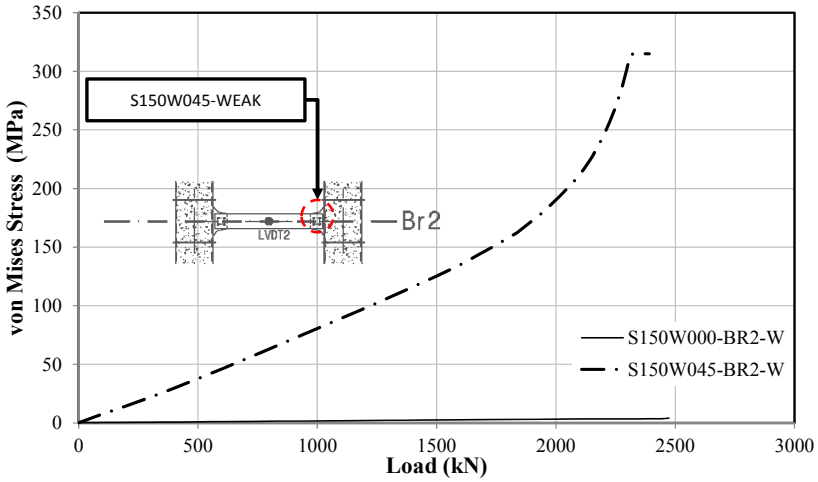

Fig. 7 Comparison of von Mises stress at BR2

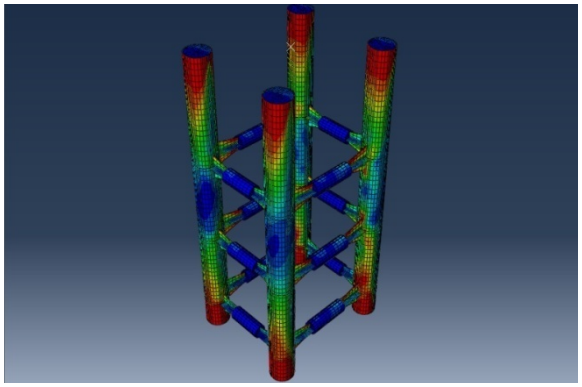

Fig. 8 Stress contour with enhanced bracing for both of the axis

Fig. 7 represents the stress-load curves at the BR2 joint. To investigate the stress concentration according to directivity at the BR2 bracing, a lateral load (150 mm, displacement control) was applied to the strong axis. The S150W000 analysis model and S150W045 model were compared to consider directivity. The S150W000 analysis model and S150W045 model showed 3.47 MPa and 314.34 MPa of von Mises stress at BR2. The results showed an 89 fold difference of stress concentration when directivity was considered relatively. To alleviate the stress concentration at bracing joints, enhanced bracing details for the weak axis need to be considered.

3.2 Enhanced bracing detail for the weak axis

To prevent premature failure at bracing joints and to alleviate the stress concentration at bracing joints, the enhanced bracing details used for the strong axis were introduced for the weak axis. Fig. 8 shows the stress contours of the analysis model with enhanced bracing of the axes.

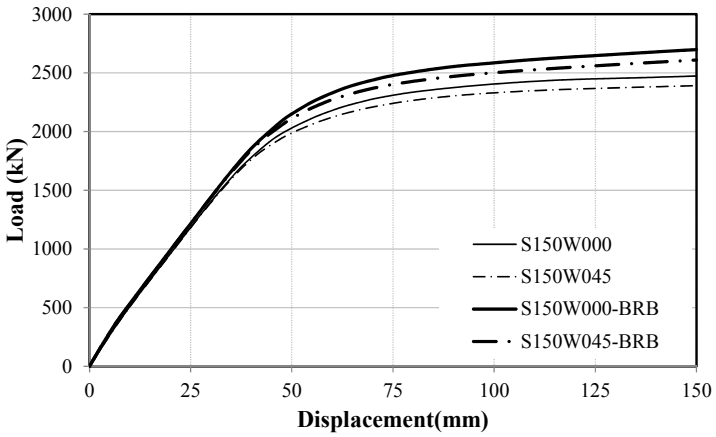

Fig. 9 Comparison of load-displacement curves for the strong axis with enhanced bracing details

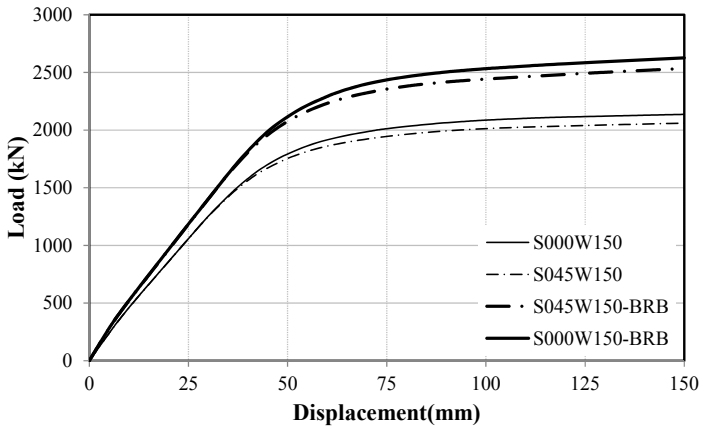

Fig. 10 Comparison of load-displacement curves for the weak axis with enhanced bracing details

Table 4 Maximum load according to enhanced bracing details

Specimen	Maximum load (kN)	Ratio (%) (S150W000)	Specimen	Maximum load (kN)	Ratio (%) (S000W150)
S150W000 (Reference specimen)	2,470	0%	S000W150 (Reference specimen)	2,140	0%
S150W045	2,390	-3%	S045W150	2,060	-4%
S150W000-BRB	2,698	9%	S000W150-BRB	2,626	23%
S150W045-BRB	2,609	6%	S045W150-BRB	2,534	19%

Figs. 9 and 10 represent the load-displacement curves for the CFT bridge pier analysis model with enhanced bracing details for both axes. In terms of the S150W000 and S150W045 models 9% and 6% increases of ultimate strength, were observed. The S000W150 and S150W000 models also showed 23% and 19% increases in ultimate strength, respectively. By using enhanced bracing details for the weak axis, global stiffness of the specimen was improved. Table 4 summarizes the analysis results with enhanced bracing details for both axes.

According to directivity, the S150W000 and S045W150 specimen showed a 17% difference in ultimate strength, while the enhanced S150W000-BRB and S045W150-BRB specimens showed a 6% difference in ultimate strength. Fig. 11 shows the load-displacement curves for the enhanced bracing detail specimen, and Table 5 shows a summary of analysis results.

By applying the enhanced bracing details on the weak axis, stress concentration at BR2 bracings was alleviated. Fig. 12 compares the von Mises stress at the BR2 bracing. Stress differences were reduced by 78% for the specimen with plate bracing on the weak axis. Table 6 summarizes the comparison results. By applying BRB bracing on the weak axis, failure at the bracing joint owing to stress concentration can be prevented.

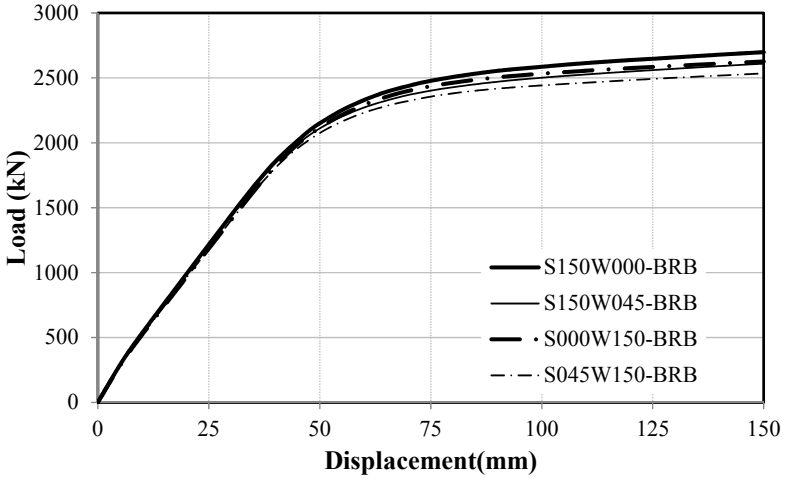

Fig. 11 Load-displacement curves for a specimen with enhanced bracing details

Table 5 Maximum load with enhanced bracing details according to directivity

Specimen	Maximum load (kN)	Ratio (%) (Before) (S150W000)	Maximum load with BRB	Ratio (%) (BRB) (S150W000)	Ratio (%) According to install BRB at weak axis
S150W000	2,470	0%	2,698 (Strong axis)	0%	9% (Strong axis)
S150W045	2,390	3%	2,609 (Stong axis)	-3%	9% (Strong axis)
S000W150	2,140	13%	2,626 (Weak axis)	-3%	23% (Weak axis)
S045W150	2,060	17%	2,534 (Weak axis)	-6%	23% (Weak axis)

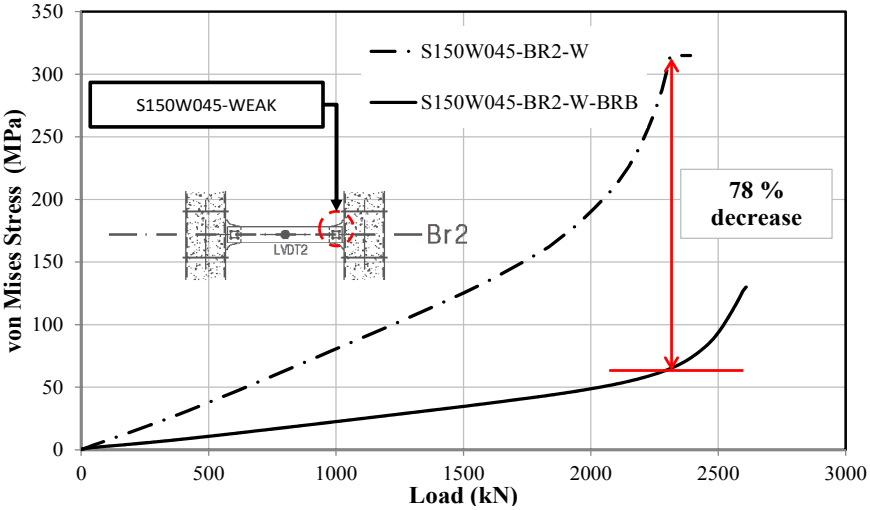

Fig. 12 Comparison of von Mises stress at BR2 connection

Table 6 Stress comparison at bracing connection with enhanced bracing of weak axis

P = 2,390 kN	Von Mises stress (MPa)	Ratio (%) (S150W045BR2-W)
S150W045-BR2-W	314.34	0
S150W045-BR2-W-BRB	69.082	22% (78% decrease)

4. Conclusions

This paper deals with new types of CFT modular bridge piers with buckling-restrained bracing. Nonlinear-finite-element analysis of CFT modular bridge piers with enhanced bracings was conducted to investigate structural performance according to directivity. From the above efforts, some common conclusions may be reached.

- CFT bridge piers with enhanced bracing details for both axes showed a 27% increase of von Mises stress compared with the reference analysis model, provided that local buckling did not occur on the CFT column. Therefore, it is expected that ductility and energy dissipation capacities are satisfied.
- Stress differences were reduced by 78% compared with the specimen with plate bracing on the weak axis. Furthermore, stress concentration at the bracing joint can be prevented by applying BRB bracing on the weak axis.
- The proposed bracing named BRB, showed improved structural performance in terms of plastic behavior for multiple CFT columns. Displacement ductility and stress concentration requirements were satisfied.

Acknowledgments

This research was supported by the Chung-Ang University Excellent Student Scholarship in 2011 and by a grant from the Construction Technology Innovation Program (10CTIPB01-Modular

Bridge Research and Business Development Consortium) funded by the Ministry of Land, Infrastructure and Transport (MOLIT) of the Korean Government.

References

Chou, C.C. and Chen, Y.C. (2006), "Cyclic tests of post-tensioned precast CFT segmental bridge columns with unbounded strands", *Earthq. Eng. Struct. Dyn.*, **35**(2), 159-175.

ElAawady, M.A. and Dawood, H.M. (2012), "Analysis of segmental piers consisted of concrete filled FRP tubes", *Eng. Struct.*, **38**, 142-152.

Ellobody, E., Young, B. and Lam, D. (2006), "Behaviour of normal and high strength concrete-filled compact steel tube circular stub columns", *J. Construct. Steel Res..*, **62**(7), 706-715.

Giakoumelis, G. and Lam, D. (2004), "Axial capacity of circular concrete-filled tube columns", *J. Construct. Steel Res.*, **60**(7), 1049-1068.

Gu, Q., Zona, A., Peng, Y. and Dall'Asta, A. (2014), "Effect of buckling-restrained brace model parameters on seismic structural response", *J. Construct. Steel Res.*, **98**, 100-113.

Hassan, M.M., Ramadan, H.M., Abdel-Mooty, M.N. and Mourad, S.A. (2014), "Behavior of concentrically loaded CFT braces connections", *J. Adv. Res.*, **5**(2), 243-252.

Hu, H., Huang, C. and Chen, Z. (2005), "Finite element analysis of CFT columns subjected to an axial compressive force and bending moment in combination", *J. Construct. Steel Res.*, **61**(12), 1692-1712.

Hu, H.T., Su, F.C. and Elchalakani, M. (2010), "Finite element analysis of CFT columns subjected to pure bending moment", *Steel Compos. Struct., Int. J.*, **10**(5), 415-428.

Kim, D.W. and Shim, C.S. (2013), "Evaluation of structural performance of precast modular pier cap" *Proceedings of 13th East Asia-Pacific Conference on Structural Engineering and Construction*, Sapporo, Japan, September, pp. 1-6.

Ma, H.W., Oh, H.C., Kim, D.W., Kong, D. and Shim, C.S. (2012), "Evaluation of flexural behavior of a modular pier with circular CFT", *J. Korean Soc. Steel Construct.*, **24**(6), 725-734. [In Korean]

MagarPatil, H.R. and Jangid, R.S. (2015), "Development and analysis of passive hybrid energy dissipation system for steel moment resisting frame", *Int. J. Civil Struct. Eng.*, **5**(4), 339-352.

Shim, C.S., Chung, Y.S. and Yoon, J.Y. (2011), "Cyclic behavior of prefabricated circular composite columns with low steel ratio", *Eng. Struct.*, **33**(9), 2525-2534.

Shim, C.S., Kim, D.W. and Kong, D. (2012), "Structural performance of precast segmental composite pier cap", *Proceedings of the 18th International Association for Bridge and Structural Engineering*, Seoul, Korea, September, pp. 611-612.

Shim, C., Kim, D., Jung, D., Kim, I. and Chung, C. (2014), "Cyclic tests of modular CFT bridge piers" *Proceedings of 10th U.S. National Conference on Earthquake Engineering Frontiers of Earthquake Engineering*, Anchorage, AL, USA, July, pp. 1-10.

Stefan, W. (2012), "Behaviour and design of generic buckling restrained brace systems", M.S. Thesis; Department of Civil and Environmental Engineering, The University of Auckland, Auckland, New Zealand.

CC